UPPSALA
UNIVERSITET

The Potential of *b*-value Variations as Earthquake Precursors for Small and Large Events

PAIBOON NUANNIN

Dissertation presented at Uppsala University to be publicly examined in Axel Hambergsalen, Geocentrum, Villavägen 16, Uppsala, Monday, May 29, 2006 at 10:00 for the degree of Doctor of Philosophy. The examination will be conducted in English.

Abstract
Nuannin, P. 2006. The Potential of *b*-value Variations as Earthquake Precursors for Small and Large Events. Acta Universitatis Upsaliensis. *Digital Comprehensive Summaries of Uppsala Dissertations from the Faculty of Science and Technology* 183. 46 pp. Uppsala. ISBN 91-554-6568-4.

The potential of variations of *b*-values in the G-R relation, $\log N = a - bM$ as earthquake precursors for small events (rockbursts) in Zinkgruvan mine, Sweden and for tectonic (large) earthquakes in the Andaman-Sumatra region were investigated.

The temporal frequency-magnitude distribution, *b(t)*, of rockbursts in Zinkgruvan mine was examined using high quality data recorded during the period November 1996 to April 2004 with magnitude ranges from $M_w = -2.4$ to 2.6. A sliding time-window was applied to compute *b*-values. The windows contain 50 events and were shifted with steps of 5 events. The results indicated that *b*-values significantly drop preceding rockbursts of magnitude $M_w \geq 1.6$.

Temporal and spatial variations of *b*-values were also examined for tectonic earthquakes, magnitude $M_w \geq 4.1$, in the Andaman-Sumatra region. Earthquake data from the ISC, IDC, NEIC and HVRD earthquake catalogs for a period from 01/01/1995 to 12/26/2004 were used for analysis. Spatial variations of *b* were calculated from circular areas containing 50 events, with nodes on a 0.5° x 0.5° grid. The analysis shows that *b(t)* estimates using data from different catalogs are comparable and that large earthquakes are preceded by a drop in *b(t)* of about 0.3~1. The distribution of stress deduced from *b*-value mapping shows that large earthquakes occurred in the high stress, i.e. low *b*-value, areas.

Aftershock sequences of the $M_w = 9$, December 26, 2004 and the $M_w = 8.7$, March 28, 2005 shocks were investigated by using the same methods. Results from aftershock sequences show similar behaviour as for the large and presumed independent main events.

The observed variations of *b*-values with time and in space support the hypothesis that *b*-values have a precursory potential. The method can be used for a wide range of earthquake magnitude, from microearthquakes ($M_w < 3$) to giant tectonic shocks ($M_w \sim 9$) and for both of independent shocks and aftershocks.

Keywords: Frequency magnitude distribution, *b*-values, rockbursts, Andaman-Sumatra region, Zinkgruvan mine, December 26, 2004 earthquake

Paiboon Nuannin, Department of Earth Sciences, Villav. 16, Uppsala University, SE-75236 Uppsala, Sweden

อุทิศแด่ พ่อ แม่ ครูบาอาจารย์ และผู้เสียชีวิตจากเหตุการณ์คลื่นยักษ์สึนามิ ๒๖ ธันวาคม ๒๕๔๗

Dedicated to my parents, my teachers and to all those who perished in the Asian Tsunami disaster of December 26, 2004.

List of papers

The thesis consists of the following four papers, which will be referred to in the text by their Roman numerals:

I   Nuannin, P., O. Kulhánek, L. Persson and K. Tillman (2002), Forecasting of increased induced seismicity in the Zinkgruvan mine, Sweden, by using temporal variations of *b*-values, Acta Montana, ser. A, No. 21(125), 13-25.

II   Nuannin P., O. Kulhánek, L. Persson and T. Askemur (2005), Inverse correlation between induced seismicity and *b*-value, observed in the Zinkruvan mine, Sweden, Acta Geodynamica et Geomaterialia, vol. 2, No. 4 (140), 5-13.

III   Nuannin P., O. Kulhánek and L. Persson (2005), Spatial and temporal *b*-value anomalies preceding the devastating off coast of NW Sumatra earthquake of December 26, 2004, Geophys. Res. Lett., 32, L11307, doi: 10.1029/2005GL022679.

IV   Nuannin P., A study of *b*-value precursors applied to the Andaman-Sumatra region, *Manuscript*.

Papers I-III have been published and are reproduced here with kind permission from the publishers. Paper IV will be submitted for publication.

Contents

Abbreviations

a	constant
b	*b*-value
b(t)	*b*-value with time
c	Seismic wave velocity
AMR	Accelerating moment release
F	The free surface correction factor
FMD	Frequency-magnitude distribution
G-R	Gutenberg-Richter relation
GUTE	Gutenberg
HRVD	Harvard CMT
IDC	International Data Center
ISC	International Seismological Centre
km	Kilometer
m_b	Body-wave magnitude
m_{max}	Maximum magnitude
m_{min}	Minimum magnitude
M	Magnitude
$\overline{M}$	Mean magnitude
M_c	Magnitude of completeness or threshold magnitude
M_o	Seismic moment
M_s	Surface-wave magnitude
M_w	Moment magnitude
N, n	Number of events
NEIC	National Earthquake Information Center
NOAA	National Oceanic and Atmospheric Administration
PAS	Seismological laboratory of the California Institute of Technology, Pasadena
WWSSN	Worldwide Standard Seismograph Network
R	Radius or distance
δb	Standard deviation of *b*-value
ΔM	Magnitude interval
Ω_o	Low frequency spectrum level
ρ	Density
$\mathscr{R}_{\theta,\phi}$	The radiation pattern coefficient

1. Introduction

Before the deployment of the WWSSN around the world in 1964, only astrologers, mystics and religious zealots were concerned with earthquake prediction. The early history of earthquake predictions featured scientists studying e.g. unusual animal behavior or watching the night skies for strange lights. Today, many respected scientists in seismology and related fields are actively working on the problem. Even when recent seismic studies provide a huge amount of new and relevant information, predictions were more often wrong than right. Increased knowledge of the earthquake source process, however, has encouraged seismologists to believe that earthquakes are preceded by phenomena that signal the coming of an earthquake within hours, days, months or years. Some encouraging indications are currently being pursued, such as anomalous ground tilt, strain changes that precede earthquakes, foreshocks, and changes in physical properties such as porosity, electrical resistivity, or elastic velocity in the hypocentral region just before rupture.

Seismic precursory phenomena, e.g. changes of seismic source parameters, seismic quiescence, accelerating moment release (AMR) and changes of the magnitude-frequency distribution of earthquakes (b-value) have been studied by previous investigators. More details will be given in Chapter 2 and 3.

This thesis is focused on the potential of the b-value, which describes the relative number of smaller and larger earthquakes in a given area, as an earthquake precursor for both small and large events i.e. for rockbursts and for natural earthquakes, respectively. The dissertation is based on four papers. In Paper I, we applied the b-value technique to earthquake tremors in the Zinkguvan mine, Sweden. In Paper II, we extended our investigation to a larger data volume when a longer time period of data became available. In Paper III, the b-value approach is employed for large earthquakes in the Andaman-Nicobar Islands and off west coast of northern Sumatra region using five-years of NEIC (USGS) catalog data preceding the M_w=9, event of December 26, 2004. Paper IV, investigates temporal and spatial variations of b-value in the Andaman-Sumatra region. Aftershock sequences of the M_w=9 (2004) and M_w=8.7 (2005) shocks were also studied. Results from four different "global" earthquake catalogs are compared. The analyses in Paper III and IV were performed by using the ZMAP software package (Wiemer, 2001).

2. Earthquake precursors

A *precursor phenomenon* is one which occurs before a mainshock and is a part of a physical preparation for the main rupture, it does not simply mean "before" but it implies casual linkage to the mainshock (Wyss and Habermann (1979). Earthquake precursor phenomena which are based on uninterrupted observation of some physical parameters like seismic wave velocity, gravity, resistivity, electricity, magnetic etc. have been frequently investigated by many authors. For example, Lu et al. (1999) observed that prior to the Tangshan, M=7.8, earthquake, resistivity recorded by nine geoelectric stations decreased within 180 km of the epicenter. During the same period, drops in water level were recorded in deep wells in the epicentral region. Apparently significant precursors in electrical resistivity data observed prior to this shock have been presented by Zhao and Qian (1994). Arabelos et.al. (2001) studied water level and water temperature changes in northern Greece, 30 km east-northeast of the city of Thessaloniki. They found a strong correlation between forthcoming earthquakes that occurred in the area and a change in the underground water level and in temperature. Meanwhile, Contadakis and Asterriadis (2001) observed changes in the underground water level and temperature in Pieria, northern Greece. They concluded that changes of underground water level and temperature can be used as earthquake precursory phenomena. Varotsos et al. (1993) described a method based on electric signals that was used for earthquake prediction in Greece. Magnetic and gravity anomalies before large earthquakes have also been studied by many authors (Eftaxias et al., 2002; Freund et al., 2004; Kushwah and Singh, 2004; Li and Wei, 1983; Ruihao et al., 1989; Song and Simons, 2003)

   Seismicity changes like e.g. seismic quiescence (periods when seismicity rate decreases to levels significantly below the normal seismicity rate), changes in the source parameters of events and changes in the frequency-magnitude distribution (FMD) have been proposed by many investigators as precursors. (Enescu and Ito, 2001, 2002; Huang et al., 2002; Monterroso and Kulhánek, 2003; Nuannin et. al., 2005; Schorlemmer et al., 2003, 2004; Wiemer et al., 2005; Wyss and Habermann, 1979; Wyss and Martirosyan, 1998). Wyss and Habermann (1988) investigated seismic quiescence before the August 1982, Stone Canyon, San Andrea Fault, earthquake and concluded that this shock could have been predicted by means of seismic quiescence. Katsumata and Kasahara (1999) used three independent earthquake

catalogs and found that the, M_w=8.3, Kurile earthquake on October 4, 1994, followed a period of outstanding seismic quiescence starting 5-6 years before the mainshock near the ruptured area. They suggest that detection of seismic quiescence is a key to the success of intermediate-term earthquake prediction. Accelerating Moment Release (AMR) preceding earthquakes with magnitude M>5 in Australia has been studied by Wang et al. (2004). They showed that 80% of the areas in which AMR occurred experienced large events. Recently, Mignan et al. (2006) demonstrated clear AMRs prior to the 26 December 2004 and to the 28 March 2005 earthquakes. They propose a model in which the AMR provides evidence that sections of Sumatra-Java were approaching failure.

Most of the methods described as successfully predicting earthquakes have been applied after the fact. It is actually quite difficult to assess if a general method of earthquake prediction is statistically successful or not. We have to specify simultaneously when, where and size. There is also a resolution problem due to the relatively large number of events necessary to reliably estimate b, and the limited number of events recorded in many areas. Large earthquakes are rather rare, and therefore there is a definite danger of "selection bias" in assessing the (statistical) success of a method. This means that it is important to compare like-with-like in a manner which is internally consistent.

3. *b*-value

The classical frequency-magnitude distribution, FMD, (Gutenberg and Richter, 1944) is commonly used, especially in association with earthquake precursors and probabilistic earthquake hazard assessments. The FMD describes the number of earthquakes occurring in a given region as a function of their magnitude *M* as:

$$\log N = a\text{-}bM \tag{1}$$

where *N* is the cumulative number of earthquakes with magnitude equal to or larger than *M*, and *a* and *b* are real constants that may vary in space and time. It should be noted that often instead of magnitude *M* the log of seismic moment or log of seismic event energy is used. The parameter *a* characterizes the general level of seismicity in a given area during the study period i.e. the higher the *a* value, the higher the seismicity. The parameter *b* is believed to depend on the stress regime and tectonic character of the region (Allen et al., 1965; Mogi, 1967; Scholz, 1968; Hatzidimitriou et al., 1985; Tsapanos, 1990). The constant *b* observed in the FMD has been taken as an indication of self-similarity at all magnitudes. If so, earthquake properties should scale uniformly in the same way from small to large earthquakes. It has been observed that the FMD may be biased by small earthquakes because the seismic moment released in small earthquakes scales differently with rupture length than it does for the large events. Another source of bias in size distributions is the saturation of earthquake magnitude for large events (Pacheco et al. 1992).

General "global" average value of the the *b* parameter, obtained by mixing different crustal rock volumes and different tectonic regimes, is close to unity. Regionally, changes in *b*-value are believed to be inversely related to changes in the stress level (Bufe, 1970; Gibowicz, 1973). An increase of applied shear stress or effective stress results in decrease of *b*-value (Urbancic et al., 1992; Wyss, 1973). A smaller *b*-value probably means that the stress is high in the examined region. Decreasing *b* within the seismogenic volume under consideration has been found to correlate with increasing effective stress levels prior to major shocks (Kanamori, 1981). Recent studies

reveal that the *b*-value is also related to the depth (Weimer and Benoit, 1996; Mori and Abercrombie, 1997; Wyss et al., 1997, 2001).

The *b*-value in eq.(1) can be estimated either by linear least squares regression or by maximum-likelihood using the equation (Aki, 1965; Ustu, 1965; Bender, 1983)

$$b = \frac{1}{\overline{M} - M_{min}} \log e \qquad (2)$$

where $\overline{M}$ denotes the mean magnitude and M_{min} the minimum magnitude of the given sample. The determination of M_{min} relies on the magnitude distribution (eq.1). In most cases, the minimum magnitude of the data set is determined by plotting the cumulative number of events as a function of magnitude (see Fig.1). These plots are then fitted with a straight line and M_{min} is the level at which the data fall below the line. The magnitude of completeness, M_c, has to be corrected by $\Delta M/2$ to compensate for the bias of rounding magnitude to the nearest ΔM bin. Therefore a correction of $M_{min}=M_c-\Delta M/2$ must be applied. More details are described by Wossener and Wiemer (2005). Generally and practically, for $\Delta M=0.1$, we assign $M_{min}=M_c$ since earthquake catalogs usually give magnitudes only with two significant digits.

An estimate of the standard deviation, δb, of the *b*-value in eq.(2) is computed by

$$\delta b = 2.30b^2 \sqrt{\sum_{i=1}^{n}(M_i - \overline{M})^2 / n(n-1)} \qquad (3)$$

(Shi and Bolt, 1982), where *n* is the total number of events of the given sample. For computing *b*-values, knowledge of completeness of a sample is important. M_c has to be computed either for every sample or defined assuming a homogenous recording quality for the entire data volume (Schorlemmer et al., 2004).

As an example, Fig. 1 shows the G-R relationship (eq.1) and the magnitude of completeness, M_c, of aftershocks of the $M_w=9$, December 26, 2004 event recorded by NEIC during the period 26/12/2004-31/12/2005. As follows from Fig.1 and eq.(1), $M_c = 4.6$, $b = 1.30\pm0.01$ and $a = 9.54$.
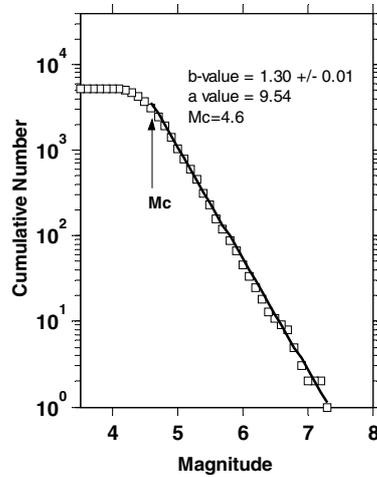
Figure 1. Frequency–magnitude distribution (FMD) of aftershocks of the 26 December, 2004 event recorded by NEIC. The slope of the line represents the Gutenberg-Richter relationship log$N$=a-bM. Complete recording is indicated by M_c (arrow).

3.1 Variations of *b*-value with time

Systematic studies have been carried out to examine the potential of temporal changes in *b*-value as a short-term, medium-term and long-term earthquake precursor. Results show that large earthquakes are often preceded by a medium-term increase in *b*, followed by a decrease in the weeks-months before the earthquake (Sammonds et al., 1992). Molchan and Dmitrieve (1990) have studied temporal *b*-value variations for foreshocks during hours-days before the mainshock. Molchan et al. (1999) found, from both regional and global earthquake catalogs, that the *b*-value of foreshocks drops by about 50%. From earthquake data for Central America from PDE and E-catalogs Monterroso (2003) found evidence that supports the hypothesis that the *b*-value decreases significantly prior to the occurrence of large earthquakes.

To study variations of *b*-value with time, a sliding time-window method is used. A group of earthquakes is chosen from an earthquake catalog. The *b*-value is calculated for the first *N* events. Then, the window is shifted by a time corresponding to certain number of events, e.g. *N*/10 events. The *b*-value is calculated for the new group of data and the process is repeated until the last event is reached. Every calculated *b*-value is assigned to the middle time of the corresponding window.

An example is displayed in Fig. 2. The *b(t)* is calculated from earthquake data in the ISC catalog using a sliding time-window containing 50 events and a 5 event shift. The choice of the number of events in the window is a compromise between the time resolution and smoothing effect of broad windows (Nuannin et al., 2005). Several tests were performed by varying the number of events in the window i.e. 75, 100 and 200. Varying the step (shift) length was also tested but it does not affect the resolution.
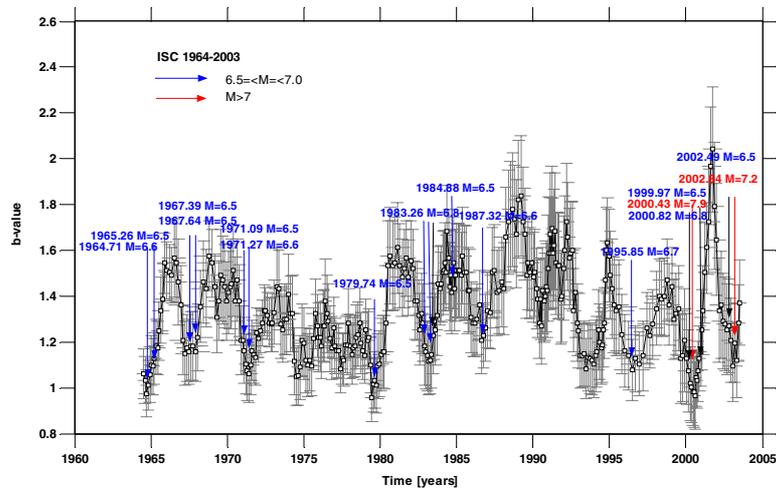

Figure 2. b(t) of the Andaman-Sumatra region during 1964-2003, data from the ISC catalog. Arrows mark the occurrence time of large events ($M_w \geq 6.5$). Vertical bars indicate standard deviation and horizontal bars indicate sample windows.

3.2 Variations of *b*-value in space

Spatial variations of *b*-value have been studied in a number of seismically active areas by other researchers. Observations of *b*-values in space reflect locally the effective stress (Scholz, 1968). Statistically significant changes of *b*-values have been observed in underground mines (Urbancic et al., 1992), and in various stress regimes such as a subducting slab (Wyss et al., 2001), along fault zones (Wiemer and Wyss, 1997b) and in aftershock zones (Wiemer and Katsumata, 1999). Gerstenberger et al (2001) used the depth distribution of *b*-values to study structural anomalies and stress level in the crust and in the upper mantle.

More recently, Monterroso and Kulhánek (2003) investigated *b*-value variations with depth in the subduction zone of Central America. They observed high *b*-values in the upper part of the slab at depths around 80-110km

beneath the volcanic chain in Guatemala-El Salvador. Nakaya (2004) analyzed seismicity data from the subducting slab along Kurile Trench. Results reveal a zone of anomalously low *b*-values near the hypocenter of the 26 September 2003, Tokachi-oki earthquake (*M*=8). Schorlemmer et al. (2004) demonstrated that *b*-value systematically varies for different styles of faulting. Normal faulting is associated with the highest *b*-values, strike-slip events show intermediate values and thrust events the lowest values. This observation means that *b* acts as a stress meter, depending inversely on the differential stress.

To map the *b*-values in space, the study area is subdivided into a grid and *b*–values are computed at every grid node within a radius contains a constant number of events (e.g. 50 events). Using this method, the radius varies with the earthquake density in space. Grid spacing may vary typically from 0.1°-1°. The resolution of a *b*-value map depends on the density of earthquakes and grid nodes, i.e. a small grid node spacing with a high density of earthquakes gives a high resolution map.

As an example, Fig. 3 shows the spatial distribution of *b*-values along the Sunda-Andaman arc in the Andaman–Sumatra region, computed with the ISC catalog from 1964 to 2003. Large earthquakes are observed in low *b*-value areas.
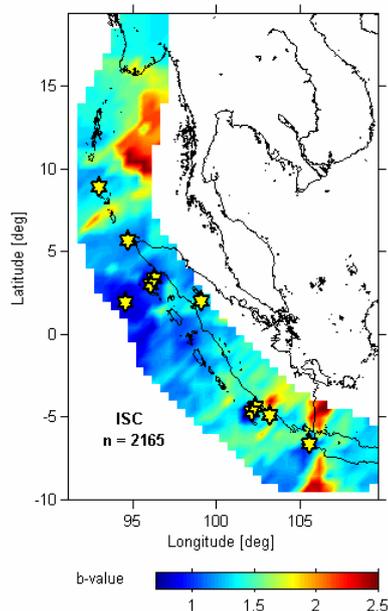

Figure 3. Distribution of *b*-value in the Andaman –Sumatra region computed with the ISC catalog 1964-2003, $M \geq M_c = 5$, $n=2,165$ events. The *b*-values are estimated from circular areas containing 50 events, centered at grid (0.5° x 0.5°) nodes. Stars mark the large earthquakes $M_w > 6.5$.

16

4. Seismicity in mines

Any underground mining activity can and most likely will generate seismic events, i.e. mining tremors, usually called rockbursts. Mining operations lead to disturbances in the natural stress field in surrounding rock masses and subsequent stress release through rockbursts takes place in volumes (within or near the mine) where the redistributed stress exceeds the strength of the rock. Rockbursts are experienced daily in many mining areas around the world e.g. in central Europe, South Africa, Australia and Canada.

Seismicity in mines has frequently been studied in order to identify precursors to intensive seismic activity in the mine. For example, Melnikov et al. (1996) demonstrated strain precursors to induced seismicity in the Khibiny apatite mines. Fajklewicz and Jakiel (1989) applied a microgravity method to predict the occurrence of mining tremors, bursts and direction of migration of increased elastic strain in the rock masses in the Pstrowski mine (Poland). They found that negative changes of gravity microanomalies signalled approaching mining tremor. Holub (1996) investigated space-time variations of the frequency-energy relation for mining-induced seismicity in the Ostrava-Karvina mine district (Czech Republic). He states that lower b-values correspond to a higher level of induced seismic activity while high b-values correspond to a low and moderate seismic activity. Kijko et al. (2001) used a non-parametric seismic hazard analysis based on the classical FMD relation (eq. 1) to estimate the maximum seismic event magnitude, m_{max}, for the Rudna copper mine in Poland and in the Western Deep Levels gold mine (the deepest mine in the world) in South Africa.

4.1 Seismic monitoring in mines

A major component in attempts to study and possibly forecast characteristics of rockbursts includes the deployment of seismic monitoring networks covering the respective mine. Such networks can detect, locate and quantify the tremors and so provide data for further analysis.

Routine seismic monitoring in mines was introduced about 40 years ago with two major objectives: Firstly, to locate major seismic events and thus guide rescue operations; Secondly, to detect the potential instabilities. In 1988, the world's first mine-worthy digital seismic data acquisition was introduced by Mendecki et al. (1990) in South Africa. The system enabled the implemen-

tation of real time quantitative seismology as a management tool for continuous monitoring of the rock mass response to mining. Seismic monitoring consists of data acquisition, seismological processing and interpretation in terms of potential for large instabilities. A seismic event is described quantitatively, apart from its timing and location. Two independent parameters pertaining to the seismic source, e.g. seismic moment and radiated seismic energy or seismic moment and stress drop, are also determined (Mendecki et al., 1996). More details are described in Paper I.

4.2 Seismic moment and moment magnitude

Seismic moment can be calculated separately from P and S waves on the basis of spectral parameters. For small seismic events ($M\sim$-2 to 4), as in the case of mining tremors, the seismic moment can be calculated from following Bruce (1970):

$$M_o = \frac{4\pi\rho c^3 R\Omega_o}{F\Re_{\theta,\phi}} \tag{4}$$

where ρ is the density of rock material, Ω_o is the low frequency spectrum level, c is either P-wave or S-wave velocity at the source, R is the distance between source and receiver, $\Re_{\theta,\phi}$ accounts for the radiation pattern coefficient for either P- or S-waves. An average value is used if the radiation pattern is not know, $\Re_{\theta,\phi}$=0.52 and 0.63 for P-waves and S-waves, respectively (Boore and Boatwright, 1984). F is the free surface correction factor. In-mine measurements, the receivers are underground. Therefore, the free surface correction is not needed. In this case, a homogeneous half space and no attenuation are assumed.

According to Hanks and Kanamori (1979), seismic moment magnitude can be determined using the scalar moment as follows

$$M_w = 2/3\log M_o - 6.1 \tag{5}$$

where M_o is in N·m.

18

5. Seismicity in the Andaman-Sumatra region

The Andaman-Sumatra region is one of the seismically most active in the world. Earthquakes that occurred in this region kill people, destroy property and cause significant damage to the economy in countries around the Bengal Bay. The most disastrous event was that of December 26, 2004, that occurred at 00:58:53 UTC (07:58:53 local time). The earthquake triggered a series of lethal tsunamis that spread throughout the Indian Ocean, killing large numbers of people and devastating coastal communities in Indonesia, Sri Lanka, India, Thailand and elsewhere. Initial estimates of the death toll were more than 280,000 people, however, more recent analysis indicates that the actual casualties were 186,983 dead, with 42,883 missing, i.e. a total of 229,886 as reported by United Nation office This catastrophe is one of the deadliest disasters in modern history. The disaster is known in Asia and in the international media as the *Asian Tsunami*, and is also called the *Boxing Day Tsunami* in Australia, Canada, New Zealand, and in the United Kingdom (http://www.tsunamispecialenvoy.org/country/humantoll.asp).

The seismic history of the Sumatra-Andaman region from the late 1600s through the early instrumental period (starting about 1900) is extensively investigated and reported in the Indonesian Journal of Natural Sciences. An important study of the seismicity of the area was made by Newcomb and McCann (1987). They found that the seismic activity of Sumatra was largely underestimated due to the lack of big earthquakes during the instrumental period. They documented two giant earthquakes during the last century: one, $M_w = 8\frac{3}{4}$, in 1833 and one, $M_w = 8\frac{1}{2}$, in 1861. They estimated that these events had rupture lengths of 550 and 300 km, respectively. They also constructed a map of source zones from historical archives for 26 historical earthquakes associated with the subduction between 1681-1921 (Rivera et al., 2002). Source areas and rupture parameters of the 1833 and the 1861 shocks and other two events which occurred in 1847, M=7, and in 1881, M=7.9, in the region were studied by Ortiz and Bilham, (2003) and by Zachariasen and Sieh (1999).

Seismicity in the Andaman-Sumatra region has been investigated by many authors (e.g., Banghar, 1987; Dasgupta and Mukhopadhyay, 1993; Dasgupta et al., 2003; Eguchi et al., 1979, Kumar et al., 1996; Sun and Pan, 1995). The paleoseismicity and seismic hazard of the Sumatra fault is investigated by Bellier et al. (1997). More recently, seismic activity in the region prior to the December 26, 2004 and the March 28, 2005 shocks was

studied by Mignan et al. (2006). Major earthquakes ($M_s \geq 7$) in the Sumatra-Andaman region during 1900-1963 are listed in Table 1 and their epicenters are depicted in Fig. 4.

Earthquakes in the region are associated with the Sunda-Andaman subduction, the Sumatra fault and a spreading zone in Andaman sea. Epicenters of earthquakes during 1973-2004 listed in NEIC catalog are shown in Fig. 5.

Table 1: *Major earthquakes ($M_s \geq 7$) that occurred in the Andaman-Sumatra region during 1900-1963. GUTE=Gutenberg, NOAA=National Oceanic and Atmospheric Administration.*

Date MM/DD/YY	Time	Lat.	Lon.	Depth (km)	Source	M_s	Catalog
2/27/1903	00:43:00	-8	106	60	NOAA	8.1	NOAA
1/4/1907	5:19:12	2	94.5	50	GUTE	7.6	PAS
6/3/1909	18:40:48	-2	101	35	GUTE	7.6	PAS
8/13/1913	4:25:42	-5.5	105	75	GUTE	7.2	PAS
6/25/1914	19:07:18	-4.5	102.5	35	GUTE	7.6	PAS
10/11/1914	16:17:06	12	94	80	GUTE	7.2	PAS
7/27/1916	11:52:42	4	96.5	100	GUTE	7	PAS
5/5/1930	13:45:57	17	96.5	35	GUTE	7.3	PAS
12/3/1930	18:51:44	18	96.5	35	GUTE	7.3	PAS
2/10/1931	6:34:25	-5.25	102.5	35	GUTE	7.1	PAS
9/25/1931	5:59:44	-5	102.75	35	GUTE	7.4	PAS
6/24/1933	21:54:46	-5.5	104.75	35	GUTE	7.5	PAS
5/1/1934	7:04:56	3.5	97.5	145	GUTE	7	PAS
8/3/1935	1:10:01	4.5	96.25	35	GUTE	7	PAS
12/28/1935	2:35:22	0	98.25	35	GUTE	7.9	PAS
1/2/1936	22:34:30	0	99.5	60	GUTE	7	PAS
8/23/1936	21:12:13	5	95	40	GUTE	7.3	PAS
9/19/1936	1:01:47	3.75	97.5	35	GUTE	7.2	PAS
6/26/1941	11:52:03	12.5	92.5	35	GUTE	8.1	PAS
4/1/1943	14:18:08	-6.5	105.5	35	GUTE	7	PAS
6/8/1943	20:42:46	-1	101	50	GUTE	7.4	PAS
6/9/1943	3:06:22	-1	101	50	GUTE	7.6	PAS
7/23/1943	14:53:09	-9.5	110	90	GUTE	7.8	PAS
11/26/1943	21:25:22	-2.5	100	130	GUTE	7.1	PAS
1/5/1944	21:12:43	-3.5	102	60	GUTE	7	PAS
5/8/1946	5:20:22	0	99.5	35	GUTE	7.1	PAS
4/16/1957	4:04:00	-4.6	107.1	546	NOAA	7.5	NOAA
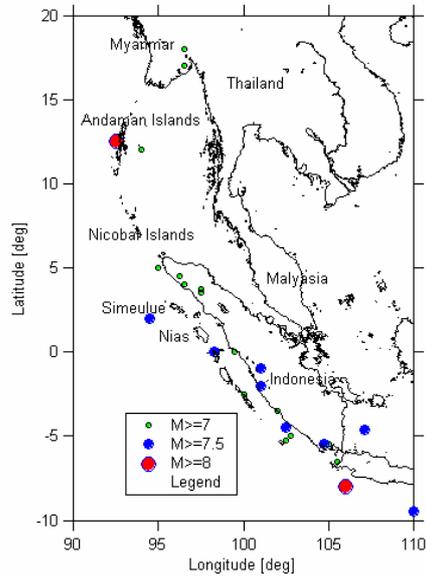
Figure 4. Epicenters of large earthquakes, $M_s \geq 7$, in the Sumatra-Andaman region during 1900-1963 (see the event list in Table 1)
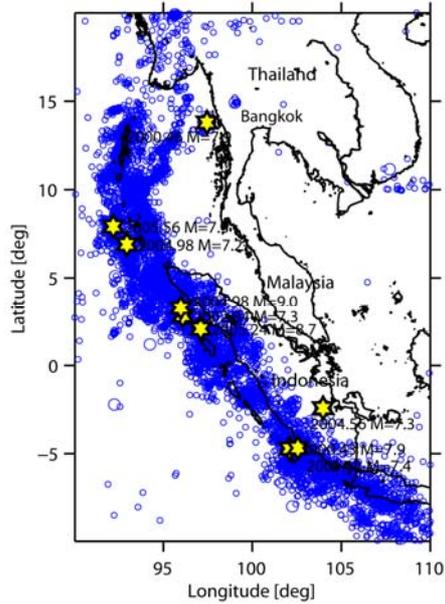

Figure 5. Epiceter map of the Sumatra-Andaman region during 1973-2004 (NEIC). Stars mark large events with magnitude $M_w > 7.0$.

6. Summary of the papers

Paper I

Rockbursts in the Zinkgruvan mine in south-central Sweden were studied. In 1996, the mine installed a digital three-dimensional seismographic network comprising 6 to 8 geophones. A panoramic location of geophones in the mine is shown in Fig. 6. During a four-year period (1996-2000), the network produced high-quality lists of rockbursts in the magnitude range from -1.6 to 2.6. 3,432 tremors were employed to determine temporal variations of *b*-values and to examine their potential as precursors to an increasing seismic activity in the mine. The *b*-value was calculated by using sliding time–windows containing 50 events. Three mining areas, defined in accordance with the observed hypocentral distribution, were studied separately (Fig.7).

Threshold magnitudes for the three areas are -0.11, -0.09 and 0.15, while the corresponding maximum magnitudes are 1.9, 2.6 and 2.4, respectively. Thus, the analysis makes use of data that span 2.0, 2.7 and 2.1 magnitude units. Calculated *b*-values show large temporal variations in a range from about 0.5 to 3.0. As an example, the *b(t)* diagram for the eastern Nygruvan area is displayed in Fig.8. There are two distinct, statistically significant (99%) drops in *b(t)*. The largest is that towards the end of 1998 for which *b*-value fell off from 1.5 to 0.8. Note, however, that the largest event taking place in the eastern Nygruvan (M_w=2.4, September 1997) was not preceded by any significant decrease of *b*.

In spite of the fact that in several cases significant decrease in *b(t)* is followed by an increase of seismic activity in the mine, a one-to-one correlation between the two phenomena has not been observed. The separation of the Zinkgruvan mine into three independent areas is, most likely, an over-simplification of the real stress field distribution. One can assume that the three areas (defined merely by the observed hypocentral patterns) are not isolated areas and that a certain degree of interconnection among them exists. If this is the case, it will complicate the deciphering of more cryptic *b(t)*-diagrams.
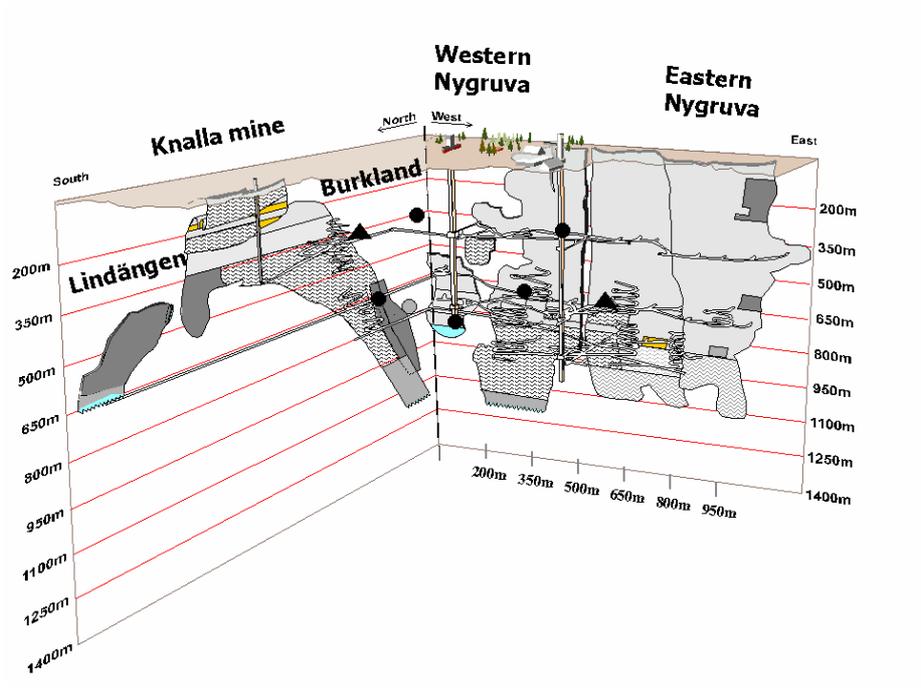
Figure 6. Panoramic view of geophone locations (circles and triangles) in the Zink-gruvan mine.
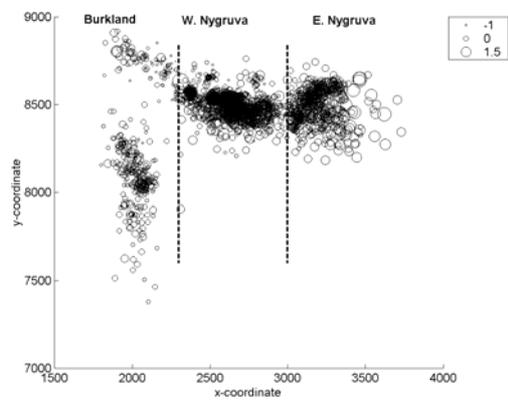
Figure 7. Horizontal projection of rockburst hypocenters in the Zinkguvan mine (November 1996-November 2000) and the division of data into three populations.
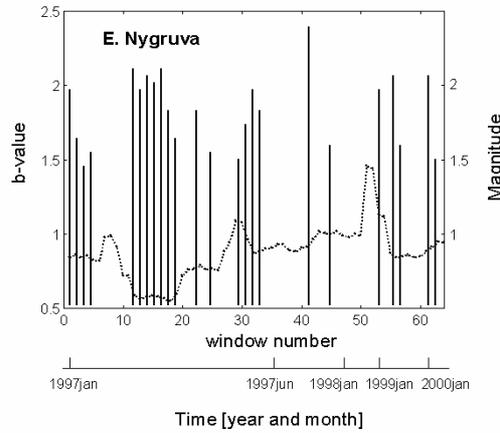
Figure 8. b(t) for eastern Nygruvan mining area. Vertical lines show the occurrence of large events $M_w \geq 1.5$.

Paper II

In Paper I, it was shown that low *b*-values can be associated with a subsequent increase of seismicity in the mine. In Paper II, we performed a similar analysis but on extended data volume covering a period from November 1996 to April 2004 and comprising 6,037 rockbursts with magnitude from -2.4 to 2.6. Frequency–magnitude distributions were studied by dividing the mine into two regions, Burkland and Nygruvan. M_c are -0.5 and -0.4 and overall *b*-values are 1.09 and 1.15 for Burkland and Nygruvan, respectively.

Figure 9 depicts the epicenters of rockbursts in the Burkland and Nygruvan ore bodies of the Zinkgruvan mine. As follows from the figure, the occruence of rockbusts in Nygruvan is higher than in Burkland.

During the reviewed time period, there are at least nine drops of *b(t)* indicated by arrows in Figure 10*(a)*. It can be seen in the figure that in several cases there is a good agreement between a sudden statistically significant decrease in the *b(t)* curve and the subsequent occurrence of large ($M_w \geq 2$) rockbursts. Figure 10*(b)* displays the seismicity of rockbursts $M_w \geq 1.6$ that occurred at time intervals following *b(t)* drops.

When compared with the results of Paper I (Fig. 8), the variation of *b*-value in Fig. 10 reveals stronger correlation between a sudden decrease in *b(t)* and a successive increase of seismicity.

24
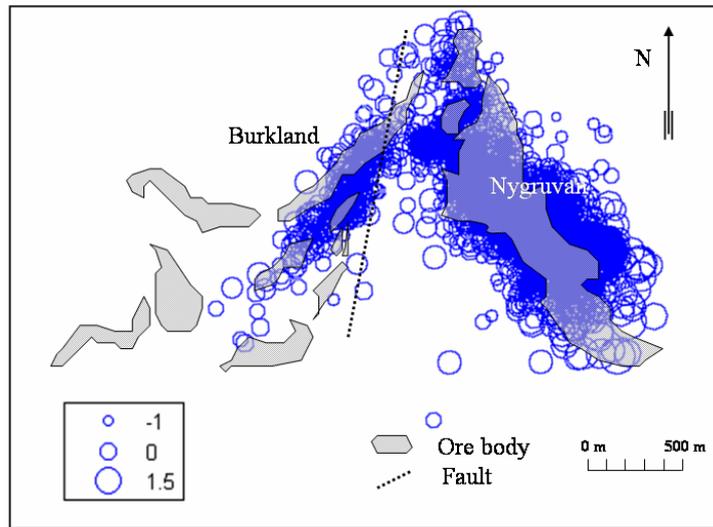
Figure 9. Epicenters of rockbursts (circles) in Nygruvan and Burkland ore bodies.
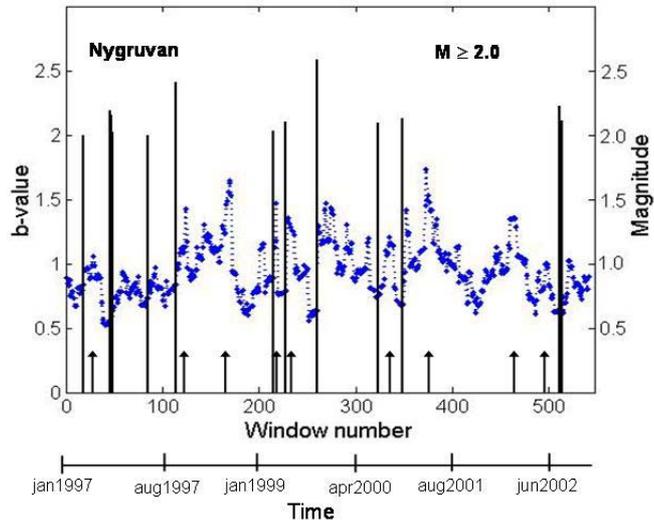
(a)
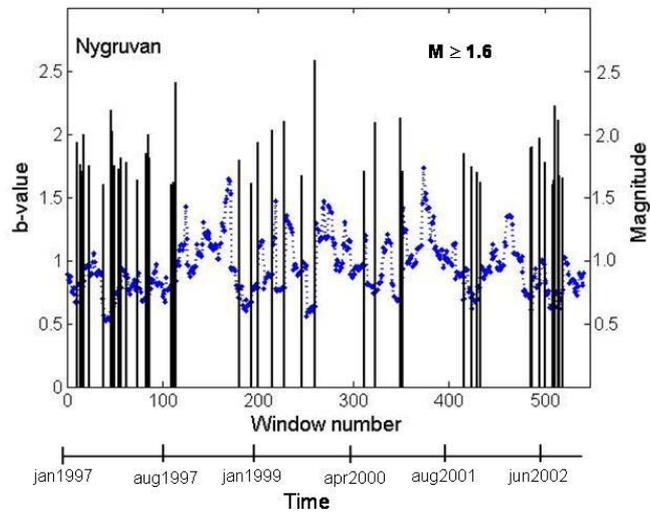
(b)

Figure 10. b-values (left scale) as a function of window number or time. Solid, vertical lines represent time of occurrence and magnitude (right scale) of all recorded rockbursts with $M_w \geq 2$ *(a)* and $M_w \geq 1.6$ *(b)*. Arrows in Fig. (a) indicate the beginning of statistically significant (99%) drops in the *b*-values.

26

Paper III

Spatial and temporal variation of *b*-values were analysed using 624 earthquakes (NEIC earthquake data) in the Andaman-Nicobar Islands region during the five-year period preceding the M_w=9 of December 26, 2004 event. Our study area was limited by latitudes 2°S-15°N and longitudes 90°W-100°E and covers the Andaman and Nicobar Islands and off west coast of northern Sumatra region. Calculations of *b* were carried out on the data listed by the USGS during the period from January1, 2000 to December 26, 2004. The incentive of the study was to examine retrospectively the potential of spatial and temporal *b*-variations as a possible precursor heralding the arrival of the giant December 26 event.

The event list was homogenized to M_s and M_w for the analysis. Body-wave magnitudes were not employed to avoid the effect of saturation. Aftershocks were manually removed from the list, leaving 611 independent events for calculations.

To examine the spatial distribution of *b*, the studied area is subdivided into 0.5°x 0.5°grids. The *b*-values are calculated for circular epicentral areas centered at grid nodes. We have chosen a constant number *N*=50 events contained within the circles. The time dependent *b*-value, *b(t)*, is calculated in sliding time-windows containing 50 events. The window is moved in 5 event steps i.e. by a 10% increment of the number of events in the window. A linear least-squares fit and magnitude increment *ΔM*=0.1 is applied throughout the work. Calculations were performed by using the ZMAP software tool package (Weimer, 2001).

Overall *b*–values with respect to M_s and M_w are, respectively 0.71 and 1.21. Two distinct drops in *b(t)* were found, one during the second half of 2002 and another towards the end of 2004. These drops can be associated with two large shocks (M_s≥7) in October and November 2002 and with the giant shock of December 26, 2004. Figure 11 depicts *b(t)* in the studied region.

The spatial distributions of *b* were also studied with respect to both M_s and M_w. Resolution maps for both cases were presented. There is a good general agreement between maps derived from the two magnitude scales. As can be seen in Fig. 12, there are no discernible differences in the northern, low *b*-value area. In the south, the anomalous low *b* extends to about 6°N and 4°N for M_s and M_w magnitudes, respectively. It implies that the accumulation of high stress prior to the M_w=9.0 shock extends approximately over an area of 450km in a NNW-SSE direction. The March 28, 2005 shock (M_w=8.7) occurred in the low *b*-value area i.e. its location correlates well with the distribution of high stresses shown in Fig. 12.
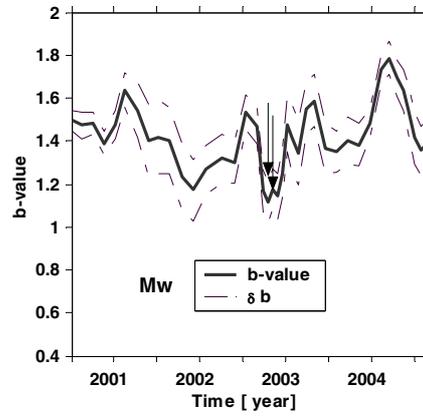
Figure 11. b(t) in the studied region (solid line) deduced with respect to M_w for a time period from January 1, 2000 to December 25, 2004. Dashed lines indicate the standard deviation and arrows mark the time occurrence of the 2002 earthquakes.
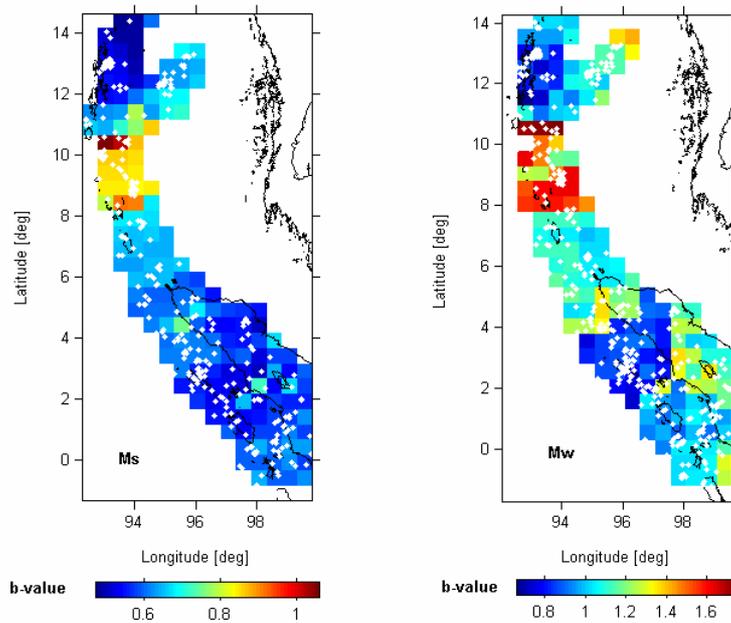

Figure 12 . Spatial distribution of *b* within the studied region. M_s (left) and M_w (right) magnitudes were used. Blue indicates low *b*, whereas red shows high *b*. White dots are epicentral location.

Paper IV

This paper is the continuation and extension of Paper III. Changes of M_c with time, variations of $b(t)$ around the epicentral area of large events, and aftershock sequences were investigated. The area is extended to 10°S-20°N and 90°-110°E covering the Andaman Islands, the Nicobar Islands and the Sumatra region. The study focuses on the determination of the b-value as a function of time and space for earthquakes in the Andaman-Sumatra region and on the assessment of its potential as an earthquake precursor.

Four earthquake catalogs have been used, ISC, IDC, NEIC and HRVD. These catalogs are different in reported magnitude scales, period of availability and number of listed events. The analysis started with magnitude homogenizing into M_w, declustering and investigation of the variation of M_c with time. Aftershock sequences of two main shocks the M_w=9, December 26, 2004 and the M_w=8.7, March 28, 2005 were investigated separately. The starting data sets used in the analysis are summarized in Table 1.

Table 2: *Parameters of catalogs used*

Catalog	Magnitude type	Time period	No. of events	*M
ISC	M_w	1/1/1964 -31/12/2003	6,876	4.2
IDC	m_b	1/1/1995-17/08/2005	13,672	3.0
NEIC	M_w	1/1/1973-31/12/2005	10,840	4.1
HRVD	M_w	1/11/977-19/11/2005	1,107	4.6

*M are chosen starting (lowest) magnitudes in the respective catalog.

Variations of b-values in both time and space were estimated using the techniques described in Chapter 3. Calculations and plots were performed using the ZMAP software tool package.

Figure 13 shows an example of the temporal variation, $b(t)$, for two five-year periods for the ISC lists. As can be seen in the figure, large earthquakes occur when b-values decrease during the study period. This phenomenon is clear in the diagrams for each catalog.
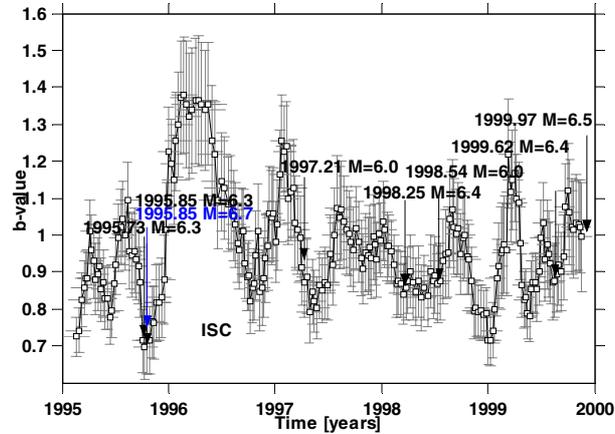
(a)
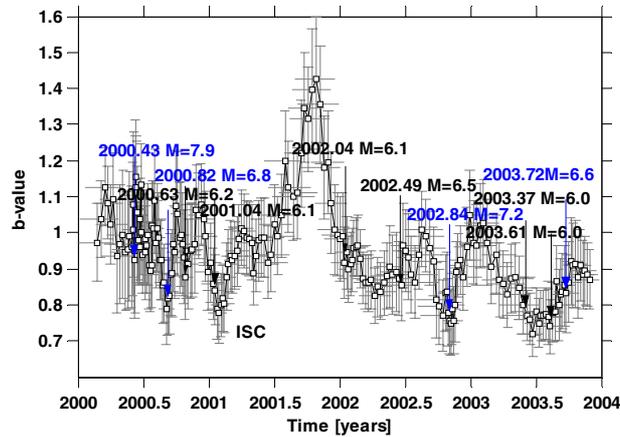
(b)

Figure 13. $b(t)$ in the study region for time period 1995-1999 (a) and 2000-2003 (b), deduced from the ISC catalog. Arrows show the occurrence of large events. Blue arrows mark events of magnitude $M_w \geq 6.6$. Vertical bars indicate one standard deviation of the b-value, horizontal bars indicate sample period.

Figure 14 displays the geographical distribution of b-values during two five-year periods, left for 1995-1999 and right for 2000-2003 (ISC data). Stars mark the epicenters of the ten largest events that occurred during each period of the analysis. All large events occurred within the low b-value $(b<1,$ dark blue/blue color) areas, with b-value ranging 0.5-1.

Two large events during the period 1995-2003 in the ISC and 1995-2004.98 for the IDC and NEIC catalogs were chosen for a detailed study of the variation of b with time in a limited area around the selected epicenters. Examples of plots of $b(t)$ are displayed in Fig. 15. It follows from the figure

that *b(t)* drops significantly prior to the occurrence of shocks in 2000 and 2002.

The rupture of the December 26, 2004 shock propagated northwards from its epicenter, from around 2°N to 15°N, i.e. from near Simeulue Island to the Andaman Islands. Nearly 3 months later, on March 28, 2005, a second large earthquake, M_w=8.7, occurred about 150 km farther southeast. Aftershock series of these two events do not overlap (Singh, 2005), lining up in opposite directions. This behavior makes it possible to distinguish the aftershocks series of the two events and to investigate separately corresponding variations of *b* in time and space. The IDC and NEIC data are used for this investigation. Figure 16 displays epicenters of aftershocks with magnitude $M \geq M_c$ of the two events.
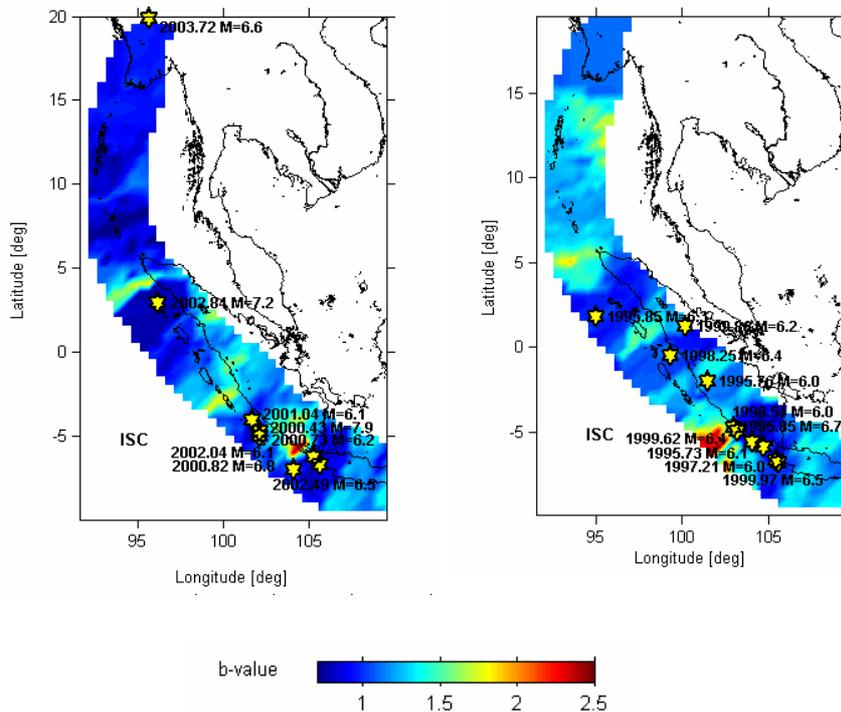
Figure 14. Spatial distribution of *b*-values for two five-year periods, i.e. 1995-1999 (left) and 2000-2003 (right) from the ISC catalog. Stars represent the 10 largest earthquakes in each period.
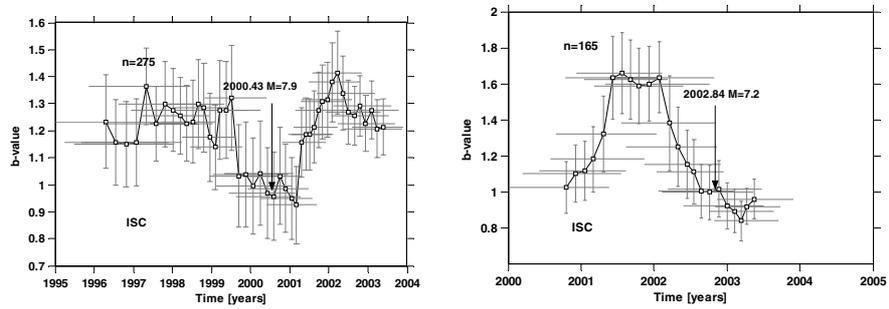
Figure 15. Temporal variations of *b*-values for an area around the two selected large events from the ISC catalog. Arrows indicate the time of occurrence of the events. *n* = number of events used. Vertical and horizontal bars show one standard deviation and sample period, respectively.
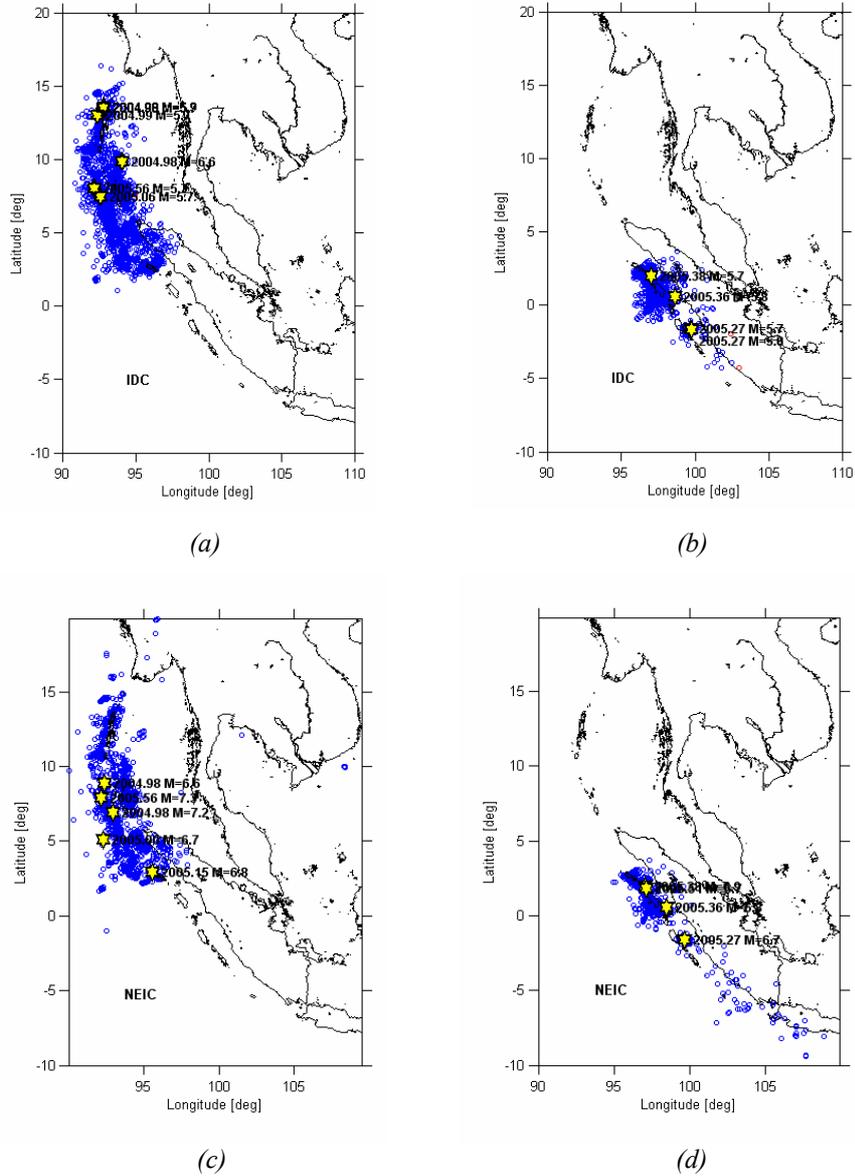
Figure 16. Epicenter map of aftershocks ($M \geq M_c$) of the two mainshocks: a), c) 26 December 2004; b), d) 28 March 2005. Stars mark large aftershocks with magnitudes $m_b > 5.6$ and $M_w > 6.5$ in the IDC and NEIC catalogs, respectively.

As an example, Fig. 17 depicts $b(t)$ of the NEIC catalog, with arrow marks showing the position of the large aftershocks. Changes of $b(t)$ before large events are significant, b changes by about 0.4-0.8 for the NEIC list. Spatial variations of b-values for the NEIC catalog are displayed in Fig. 18.

33
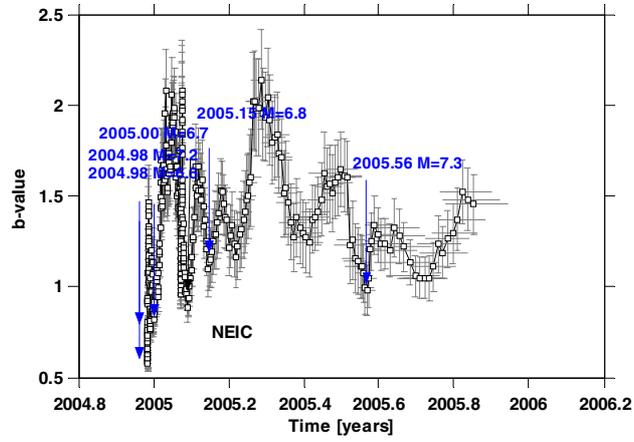
(a)
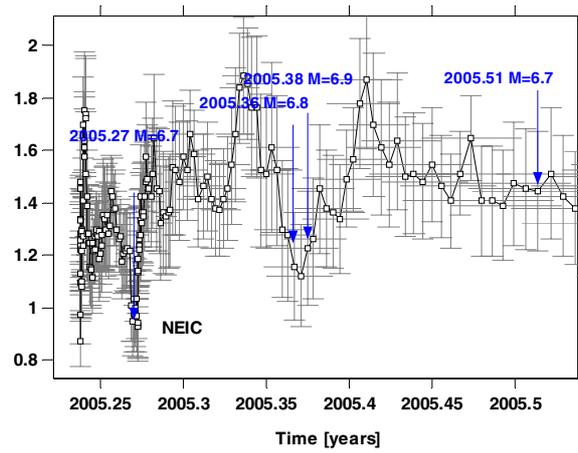
(b)

Figure 17. b(t) of the aftershocks for the NEIC catalog: *a)* the event of December 26, 2004 ; *b)* the event of March 28, 2005
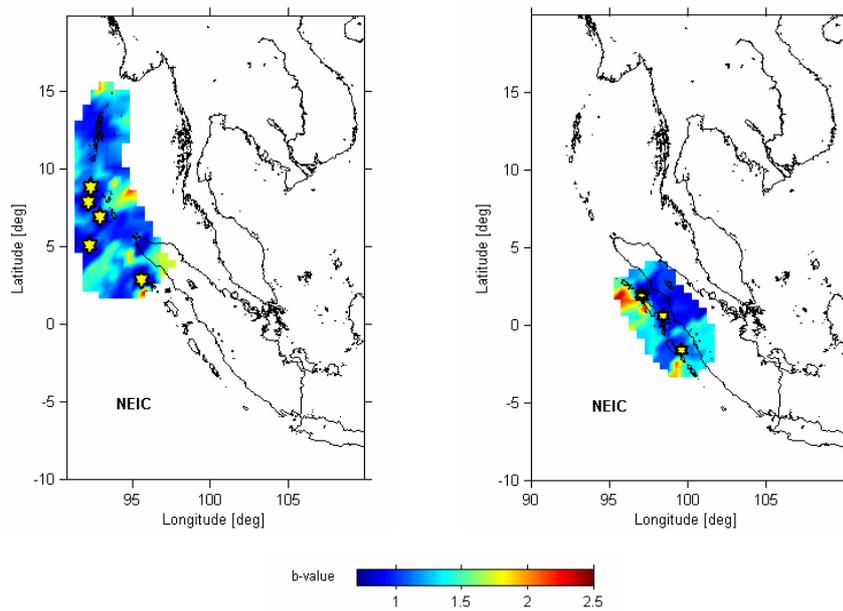
Figure 18. b-value maps of two aftershock sequences (NEIC data). Left: aftershocks of the December 26, 2004 event. Right: aftershocks of the March 28, 2005 event. Stars mark large aftershocks with magnitude M_w>6.5.

7. Conclusions

The concept of variations of *b*-values in time as earthquake precursors was successfully applied for rockbursts in Zinkgruvan mine, Sweden and for tectonic earthquakes in the Andaman-Sumatra region. Results reveal that large earthquakes occur during low *b*-value time intervals.

In Paper I, rockbursts with magnitude ranging from $M_w = -1.6$ to 2.6 were used for *b*-value determination as a function of time. Three mining areas were studied separately. Statistically significant drops in *b(t)* can be associated with subsequent increase of seismicity. Two large rockbursts were not preceded by any significant decrease of *b*. In general, drops in *b* values reveal an U-shape curve in the *b(t)* diagrams. Most of the associated seismicity takes place close to the minima in the *b(t)*-curve. The three regions studied show similar results.

In Paper II, *b(t)* is determined from rockbursts recorded during a 7-year period, and with magnitudes ranging from $M_w = -2.4$ to 2.6. Calculated *b*-values show large time variations between 0.6 and 1.8. Almost all statistically significant drops in *b*-value can be associated with an occurrence of large shocks ($M_w \geq 1.6$) in the mine, either as isolated events or as a sequence of several shocks. Results form Paper I and II, indicate that variation of *b(t)* for small events like rockbursts (magnitude range from $M_w = -2.4$ to 2.6) can be used as a rockburst precursor.

In Paper III, we investigated variations of *b*-values for tectonic earthquakes with magnitude ranging from $M_w = 3.8$ to 7.1 during a five-year period prior to the $M_w = 9$, December 26, 2004 shock. *b(t)* varied in a broad range from 1.10 to 1.78. Statistically significant drops in *b* associated with the time occurrence of two large events ($M_s \geq 7$) in 2002 and with the giant shock towards the end of 2004 are observed. *b*-value mapping indicates the region of stress concentration (low *b*-value areas). A low *b*-value anomaly, around the $M_w = 9$, (2004) and $M_w = 8.7$, (2005) events supports the hypothesis that rupture will occur in high stress (low *b*) areas.

The study of *b*-value with time and in space used in Paper III is extended to a larger area, longer time period and different earthquake catalogs in Paper IV. Variations in *b(t)* for two consecutive five-year periods ranging from 0.7-1.4, 0.5-2, 0.75-1.40 and 0.75-1.35 for the ISC, IDC, NEIC and HRVD catalogs, respectively were observed. Results show that large events occurred in intervals of low *b* values. A rapid increase of *b(t)* is observed after

the occurrence of large earthquakes. This typical phenomena is observed in *b(t)* plots for most of the large earthquakes.

b-value mapping is a useful tool to display variation of stress accumulation over large areas. Generally, it follows from Paper III that large earthquakes occurred in high stress areas (low *b*) and no large earthquake took place in high *b* areas.

Variations of *b(t)* for the aftershock series of the M_w=9 and the M_w=8.7 events were studied. Distributions of *b* show that large shocks occurred in low *b* areas for both aftershock series.

Results from the present study suggest that changes of *b*-value have a potential to be used as earthquake medium-term (months-years) precursors for small and large events (M_w=-2.4-9) and as short-term (days-months) precursors for aftershock series. Precursory time or resolution of *b(t)* depends on the detection ability of the network. Therefore, local or regional networks are likely to provide a higher resolution. In order to make warning appropriate and efficient, *b*-values monitoring in both time and space are necessary. Hence, a real time software tool package needs to be developed, especially to allow web-based application.

Summary in Swedish

I denna avhandling har variationer i b-värdet från G-R relationen undersökts och använts som förelöpare och indikator för gruvskalv i Zinkgruvan i Närke, Sverige, och jordskalv i Andaman-Sumatra området i Sydostasien. b-värdets variation som funktion av tiden, $b(t)$, har studerats i Zinkgruvan under perioden 1996 till 2004 inom magnitudområdet -2.4 till 2.6. Beräkningen har utförts med hjälp av ett glidande fönster baserat på vardera 50 skalv som successivt flyttats i steg av 5 skalv. De data som användes i dessa undersökningar är inspelat med ett lokalt nätverk installerat i gruvans närområde.

Resultaten visar att b-värdet signifikant minskar innan ett större gruvskalv sker ($M_w \geq 1.6$). Vidare undersöktes b-värdets temporala och spatiala variationer för tektoniska jordbävningar med magnitud $M_w \geq 4.1$ i Andaman-Sumatra regionen. I denna undersökning användes fyra olika kataloger, ISC, IDC, NEIC och HVRD, i tidsperioden 01/01/1995 till 26/12/ 2004. För de temporala variationerna användes samma fönsterlängd och steg som i gruvskalvsundersökningen. Den spatiala variationen beräknades i en grid med hjälp av cirkulära fönster där dess arealstorlek begränsas av cirkeln med radien innefattande 50 skalv i varje fönster. Resultaten visar att de temporala variationerna i b-värdet är jämförbara mellan de fyra olika katalogerna och påvisar att stora skalv sker när b-värdet faller signifikant med 0.3 till 1. Den spatiala fördelningen av b-värden påvisar hur stora jordskalv sker i områden med hög spänning och lågt b-värde.

Vidare har två efterskalvssekvenser studerats, dels efter det stora skalvet 26/12/2004, M_w=9, och ett skalv 28/03/2005, M_w=8.7. Denna studie utfördes med samma metod som ovan och påvisar att egenskaperna i b-värdet är jämförbara för grupper med beroende händelser som med oberoende händelser. Sammanfattningsvis kan sägas att denna studie påvisar att förändringar i b-värdet både temporalt och spatialt kan användas för förutsägelser av jordskalv.

Det ger indikationer på månader upp till år för små skalv ($M_w \sim 3$) till stora skalv ($M_w \sim 9$) och dagar upp till månader för efterskalv. Upplösningen i tiden ges av känsligheten i nätverket som har producerat katalogen. Om jordskalförutsägelser skall göras operativt och effektivt krävs ett webbaserat system som har möjlighet att fungera i nära realtid och kan ge förutsägelser både temporalt och spatialt.

Acknowledgements

My respectful thanks go to my father, mother, brothers and sisters who always support me and look forward to my homecoming every time I return from Uppsala. Last but not least, I am very much indebted to my wife, Kanya and Theerakarn (Junior) my only lovely son for their patience whenever I have been away from home.

In Thailand

I would like to thank:

Department of Physics, Faculty of Science, Prince of Songkla University, PSU, and all my colleagues who had to shoulder my teaching load, especially, Geophysics members, Assist. Prof. Dr. Warawutti Lohawijarn and Asist. Prof. Dr. Tripob Bhongsuwan. Assoc. Prof. Dr. Thawat Chittrakarn, Dean of Faculty of Science for his kind permission for a leave of absence, executive team who carried on my duty when I was absent from the office. Assoc. Prof. Dr. Sunthorn Sotthibandhu for his invaluable stimulation with *"break a rice cooking pot (set aside everything else and never be wavered), then go to Uppsala and won't be back until the thesis is completed"*. Dr. Chatchalit Rattarasarn (M.D.) and Dr. Methinee Rattarasarn for a physical examination and healthcare consultant. Rachanee Sunyiwa, Rambhai Juthaporn and Sudarat Kovutikulrangsee who have prepared all official documents for getting permission from PSU and for passport application. Urai Umpama, Choosri Meesupree, Jiratha Chouykaew who prepared ingredients for my Thai cooking in Uppsala. Sathaporn Suwan for *"Looktung"* song entertainment and problem solving for PC program that I used remotely. All of my relatives, friends and villagers at Ban Thoongpoh, Namom District. Reservation staffs of Thai Airways International, Hatyai office for their helpfulness in making a seat available whenever I traveled to Sweden.

In Sweden

I am grateful to:

Dynesius's family: Lars, Lena, Linn and Louis and Harley's family, my host family, Thomas and Eva for their help and warm hospitality when I first came to Uppsala in 1989, they made me feel at home. Siv Petterson, Conny Holmqvist and Leif Nyberg for technical assistance and fuzzy works. Susanne Ehlin, Platschef of Earth Sciences Library for introducing me how to use an electronic library. All *doktorand* friends for sharing both of academic and generous experiences while I was studying in seismology at Department of Earth Sciences, Uppsala University. Thai friends for sharing valuable time for cooking, shopping and sightseeing. Mr. Bundit Saralamba, managing director, Thai Airways International, Stockholm office for allowing me to carry an excess luggage back home.

40

References

Aki, K. (1965), Maximum lilkelihood estimate of *b* in the formula log*N=a-bM* and its confidence limits, Bull. Earthq. Res. Inst., 43, 237-239.

Allen, C., P. Amand, C. Richter and J. Nordquist (1965), Relation between seismicity and geological structure in the southern California region, Bull. Seismol. Soc. Am., 55, 752-797.

Arabelos, D., G. Asteriadis, M. Contadakis, G. Zioutas, D. Xu, C. Zhang, and B. Zheng (2001), The use of an outlier detecting method in time series of continuous daily measurements of underground water level and temperature in earthquake prediction investigation, Tectonophysics, 338, 315-323.

Banghar, A.R. (1987), Seismo-tectonics of the Andaman-Nicobar Islands, Tectonophysics, 133, 95-104.

Bellier, O., M. Sebrier, S. Pramumijoyo, Th. Beaudouin, H. Harjono, I. Bahar and O. Forni (1997), Paleosiesmicity and seismic hazard along the great Sumatran fault (Indonesia), J. Geodynamics, 24(1-4), 169-183.

Bender, B. (1983), Maximum likelihood estimation of *b* values for magnitude grouped data, Bull. Seismol. Soc. Am., 73(3), 831-851.

Boore, D.M., and J. Boatwright (1984), Average body-wave radiation coefficients, Bull. Seismol. Soc. Am., 74(5), 1,754-1,782.

Brune, J.N. (1970), Tectonic stress and the spectra of seismic shear waves from earthquakes, J. Geophys. Res., 75, 4,997-5,009.

Bufe, C.G. (1970, Frequency-magnitude variations during the 1970 Danville earthquake swarm, Earthquake Notes, 41, 3-6.

Contadakis, M. E., and G. Asteriadis (2001), Recent results of the research for preseismic phenomena on the underground water and temperature in Pieria, northern Greece, Nat. Hazards and Earth System. Sci., 1, 165-170.

Dasgupta, S., and M. Mukhopadhyay (1993), Seismicity and plate deformation below the Andaman arc, northeastern Indian Ocean, Tectonophysics, 225, 529-542.

Dasgupta, S., M. Mukhopadhyay, A. Bhattacharya and T.K. Jana (2003), The geometry of the Burmese-Andaman subducting lithosphere, J. Seismology, 7, 155-174.

Eftaxias, K., P. Kapiris, E. Dologlou, J. Kopanas, N. Bogris, G. Antonopoulos, A. Peratzakis, and V. Hadjicontis (2002), EM anomalies before the Kozani earthquake: A study of their behavior through laboratory experiment, Geophys. Res. Lett., 29(8), 10.1029/2001GL013786.

Eguchi, T., S. Ueda and T. Maki (1979), Seismotectonics and tectonic history of the andaman sea , Tectonophysics, 57, 35-51.

Enescu, B., and K. Ito (2001), Some premonitory phenomena of the 1995 Hyogo-Ken Nanbu (Kobe) earthquake: seismicity, *b*-value and fractal dimension**,** Tectonophysics*, 338 (3-4) , 297-314.

Enescu, B., and K. Ito (2002), Spatial analysis of the frequency-magnitude distribution and decay rate of the 2000 Western Tottori earthquake, Earth Planets Space, 54(8), 847-860.

Fajklewicz, Z., and K. Jakiel (1989), Induced gravity anomalies and seismic energy as a basis for prediction of mining tremors, PAGEOPH, 129(3/4), 536-552.

Freund, F.T., A. Takeuchi, B.W.S Lau, and C.G. Hall (2004), Positive holes and their role during the build-up of stress prior to the Chi-Chi Earthquake, Int. Conf. in Commemoration of 5th Anniversary of the Chi-Chi Earthquake Taipei, Taiwan.

Gerstenberger, M., S. Wiemer, D. Giardini (2001), A systematic test of the hypothesis the b-value varies with depth in California, Geophys. Res. Letts., 28(1), 57-60.

Gibowicz, S.J. (1973), Variation of the frequency-magnitude relation during earthquake sequences in New Zealand, Bull. Seismol. Soc. Am., 63, 517-528.

Gutenberg, B., and C. Richter (1944), Frequency of earthquakes in California, Bull. Seismol. Soc. Am., 34, 185-188.

Hanks, T.C., and H. Kanamori (1979), A moment magnitude scale, J. Geophys. Res., 84, 2348-2350.

Hatzidimitriou, P., D. Papadimitriou Mountrakis and B. Papazachos (1985), The seismic parameter b of the frequency-magnitude relation and its association with the geological zones in the area of Greece, Tectonophysics, 120, 141-151.

Holub, K. (1996), Space-time variations of the frequency-energy relation for mining-induced seismicity in the Ostrava-Karvina mining district, PAGEOPH, 146, 265-280.

Huang, Q., A.O. Öncel, and G.A. Sobolev (2002), Precursory seismicity changes associated with the M_w=7.4 1999 August 17 Izmit (Turkey) earthquake, Geophys. J. Int., 151, 235-242.

Kanamori, H. (1981), The nature of seismic patterns before large earthquakes. In Earthquake Prediction: An International Review (eds. Simpson, D.W., and Richards, P.G.)(Maurice Ewing Series, vol.4, AGU, Washington D.C., 1-19.

Katsumata, K., and M. Kasahara (1999), Precursory seismic quiescence before the 1994 Kurile Earthquake (Mw=8.3) revealed by three independent seismic catalogs, Pure Appl. Geophys., 155, 443-470.

Kijko, A., S. Lasocki, and G. Graham (2001), Non-parametric seismic hazard in mines, Pure Appl. Geophys., 158, 1,655-1,675.

Kumar Ravi, M., N. Purnachandra, and S.V. Chalam (1996), A seismotectonic study of the Burmar and Andaman arc regions using centroid moment tensor data, Tectonophysics, 253, 155-165).

Kushwah V. K., and B. Singh (2004), Initial results of ultra low frequency magnetic field observations at Agra and their relation with seismic activities, Current Science, 87(3), 332-339.

Li, M., and Z. Wei (1983), Gravity variation before and after Tangshan earthquake, Tectonophysics, 97, 158.

Lu, J., F. Qian, and Y. Zhao (1999) Sensitivity analysis of the Schlumberger monitoring array: application to changes of resistivity prior to the 1976 earthquake in Tangshan, China , Tectonophysics, 307, 397-405.

Melnikov, N. N., A. A. Kozyrev, and V. I. Panin (1996), Induced seismicity in large-scale mining in the Kola Peninsula and monitoring to reveal informative precursors, PAGEOPH, 147(2), 263-276.

Mendecki, A.J., G. van Aswegen, J.N.R. Brown, and P. Hewlett (1990), The Welcom Seismological network, Proc. 2nd International Symposium on Rockburst and Seismicity in Mines, Minneapolis. 367-377.

Mendecki, A.J., A. van Z. Brink, R.W.E. Green, P. Mountfort, A. Dzhafarov, J. Niewiadomski, A. Kijko, M. Sciocatti, S. Radu, G. van Aswegen, P. Hewlett, E de Kock, and T. Stankiewicz (1996), Seismology for rockbursts prevention, control and prediction, SIMRAC report, ISS International Limited, 309 pp.

Mignan, A., G. King, D. Bowman, R. Lasscassin, and R. Dmowska (2006), Seismicity in the Sumatra-Java region prior to the December 26, 2004 (M_w 9.0-9.3) and March 28, 2005 (M_w=8.7) earthquakes, Earth and Planet. Sci. Lett., (in press).

Mogi, K. (1967), Regional variation in magnitude-frequency relation of earthquake, Bull. Earthq. Res. Inst., 45, 313-325.

Molchan. G.M., and O. Dmitrieve (1990), Dynamics of magnitude-frequency relation of foreshocks, Phys. Earth Planet. Inter., 61, 99-112.

Molchan, G.M., T.L. Kronrod, and A.K Nekrasova (1999), Immediate foreshocks: time variation of the *b*-value, Phys. Earth Planet. Inter., 111, 229-240.

Monterroso, D. (2003), Statistical seismology studies in Central America: *b*-value, seismic hazard and seismic quiescence, Compr. Summaries Uppsala Diss. Fac. Sci. Technol. 897, 27 pp., Acta Univ. Upsaliensis, Uppsala, Sweden.

Monterroso, D.A., and O. Kulhánek (2003), Spatial variations of *b*-values in the subduction zone of Central America, Geofisica Int., 42(4), 1-13.

Mori, J., and R.E. Abercrombie (1997), Depth dependence of earthquake frequency-magnitude distributions in California: Implication for the rupture initiation, J. Geophys. Res., 102, 15,081-15,090.

Nakaya, S., (2004), A zone of anomously low *b*-value within the subduction slab prior to the September 26, 2003, Tokachi-oki, Japan, earthquake (M=8.0), EOS Trans. AGU, 85(47), Fall Meet. Suppl., Abstract S13A-1028.

Nuannin, P., O. Kulhánek, and L. Persson (2005), Spatial and temporal *b*-value anomalies preceding the devastating off coast of NW Sumatra earthquake of December 26, 2004, Geophys. Res. Lett., 32, L11307, doi:10.1029/2005GL022679.

Newcomb, K.R., and W.R. McCann (1987), Seismic history and seismotectonics of the Sunda arc, J. Geophys. Res. 92(B1), 421-439.

Ortiz, M. and R. Bilham (2003), Source area and rupture parameters of the 31 December 1881 M_w=7.9 Car Nicobar earthquake estimate from tsunamis recorded in the Bay of Bengal, J. Geophys. Res., 108, 2,215-2,230.

Pacheco, J.F., C. H. Scholz, and L.R. Sykes (1992), Change in frequency-size relationship from small to large earthquakes, Nature, 355, 71-73.

Rivera, L., K. Sieh, D. Helmberger, and D. Natawidjaja (2002), A Comparative Study of the Sumatran Subduction-Zone Earthquakes of 1935 and 1984, Bull. Seismol. Soc. Am., 92(5), 1721-1736.

Ruihao, L., S.Heping, and H. Yenchang (1989), Investigation of gravity variation associated with crustal deformation of the Tianjin area before and after the Tangshan Earthquake, Tectonophysics, 167, 431-347.

Sammonds, P.R., P.G. Meredith, and I.G. Main (1992), Role of pore fluid in the generation of seismic precursors to shear fracture, Nature, 359, 228-230.

Scholz, C.H. (1968), The frequency-magnitude relation of micro-fracturing in rock and its relation to earthquakes, Bull. Seismol. Soc. Am. 58, 399-415.

Schorlemmer, D., G. Neri, S. Wiemer, and A. Mostaccio (2003), Stability and significance tests for *b*-values anomalies: example from the Tyrrhenian Sea, Geophys. Res. Lett., 30 (16), 1835, doi10.1029 /2003GL017335.

Schorlemmer, D., S. Wiemer, and M. Wyss (2004), Earthquake statistics at Parkfield I: Stationarity of *b*-values, J. of Geophys. Res. 109, B12307, doi10.1029 /2004-JB003234.

Shi, Y., and B.A. Bolt (1982), The standard error of the magnitude-frequency *b*-value, Bull. Seismol. Soc. Am., 72, 1677-1687.

Singh, S.C. (2005), Sumatra earthquake research indicates why rupture propagated northward, EOS, Trans., AGU, 86(48), 497-502.

Song, Teh-Ru A., and M. Simons (2003), Large trench-parallel gravity variations predict seismogenic behavior in subduction zones, Science, 301, 630-632.

Sun, J., and T. Pan (1995), Seismic characteristics of Sumatra and its relevance to Peninsular Malaysia and Singapore, J. Southeast Asian Earth Sci., 12, 105-111.

Tsapanos, T. (1990), *b*-value of two tectonic parts in the circum-Pacific belt, PA-GEOPH, 143, 229-242.

Urbancic, T. I., C-I. Trifu, J. M. Long, and R.P. Young (1992), Space-time correlation of *b* values with stress release, PAGEOPH., 139 (3/4), 449-462.

Ustu, T. (1965), A method in determining the value of *b* in a formula log*n =a-bM* showing the magnitude frequency for earthquakes. Geophys. Bull. Hokkaido Univ., 13, 99-103.

Varotsos, P., K. Alexopoulos and M. Lazaridou (1993), Latest aspects of earthquake prediction in Greece based on seismic electric signals, II**,** Tectonophysics, 224, (1-3), 1-37.

Wang, Y., C. Yin, P. Mora, X. Yin, and K. Peng (2004), Spatio-temporal scanning and statistical test of the accelerating moment release (AMR) model using Australian earthquake data, Pure Appl. Geophys., 161, 2281-2293.

Wiemer, S. (2001), A software package to analyze seismicity: ZMAP, Seismol. Res. Lett., 72, 373-382.

Wiemer, S., and J. Benoit (1996), Mapping the *b*-value anomaly at 100 km depth in the Alaska and New Zealand subduction zones, Geophys. Res. Lett., 23, 1557-1560.

Wiemer, S., and K. Katsumata (1999), Spatial variability of seismicity parameters in aftershock zones, J. Geophys. Res., 104 (13), 13,135-13,151.

Wiemer, S., and M. Wyss, (1997) Mapping the frequency-magnitude distribution in asperities: An improved technique to calculate recurrence times?, J. Geophys. Res., 102, 15,115-15,128.

Wiemer, S., A. Yoshida, K. Hosono, S. Nogichi, and H. Takayama (2005), Correlating seismicity parameters and subsidence in the Tokai region, central Japan, J. Geophys. Res., 110, B10303, doi: 10.1029/2003JB002732.

Wossener, J., and S. Wiemer (2005), Assessing the quality of earthquake catalogues: estimating the magnitude of completeness and its uncertainty, Bull., Seismol. Soc. Am., 95(2), April, doi10.1785/0120040007.

Wyss, M., (1973), Towards a physical understanding of earthquake frequency distribution. Geophys. J. R. astron. Soc., 31, 341– 359.

Wyss, M., and R. E. Habermann (1979), Seismic quiescence precursory to a past and a future Kurile island earthquake, Pure Appl. Geophys., 117, 1195-1211.

Wyss, M., and R.E. Habermann (1988), Precursory quiescence before the August 1982 Stone Canyon, San Andrea Fault, earthquakes, PAGEOPH., 126(2-4), 333-356.

Wyss, M., and A. H. Martirosyan (1998), Seismic quiescence before the M 7, 1988, Spitak earthquake, Armenia, Geophys. J. Int., 134(2), 329-340.

Wyss, M., K. Shimazaki, and S. Wiemer (1997), Mapping active magma chambers by *b*-value beneath the off-Ito volcano, Japan, J. Geophys. Res., 102, 20413-20422.

Wyss, M., F. Klein, K. Nagamine, and S. Wiemer (2001), Anomalously high *b*-values in the South Flank of Kilauea volcano, Hawaii: evidence for the distribu-

tion of magma below Kilauea's East rift zone, J. Volcan. Geotherm. Res., 106, 23-37.

Zachariasen, J., and K. Sieh (1999), Submergence and uplift associated with the giant 1833 Sumatran subduction earthquake: evidence from coral microatolls, J. Geophys. Res., 104, 895-919.

Zhao, Y., and F. Qian (1994), Geoelectric precursors to strong earthquakes in China, Tectonophysics, 233(1–2), 1994, 99–113.